Preparation and Properties of α-Chitin-Whisker-Reinforced Hyaluronan–Gelatin Nanocomposite Scaffolds

Parintorn Hariraksapitak,* Pitt Supaphol

Petroleum and Petrochemical College and Center for Petroleum, Petrochemicals, and Advanced Materials, Chulalongkorn University, Bangkok 10330, Thailand

Received 3 September 2009; accepted 8 January 2010
DOI 10.1002/app.32095
Published online 12 May 2010 in Wiley InterScience (www.interscience.wiley.com).

ABSTRACT: Tissue scaffolds made of naturally derived polymers present poor mechanical properties, which may limit their actual utilization in certain areas where high strength is a key criterion. This study was aimed at developing tissue scaffolds from a 50 : 50 w/w blend of hyaluronan (HA) and gelatin (Gel) that contained different amounts of acid-hydrolyzed α-chitin whiskers (CWs) by a freeze-drying method. The weight ratios of the CWs to the blend were 0–30%. These scaffolds were characterized for their physical, physicochemical, mechanical, and biological properties. Regardless of the CW content, the average pore size of the scaffolds ranged between 139 and 166 μm. The incorporation of 2% CWs in the HA–Gel scaffolds increased their tensile strength by about two times compared to those of the other groups of the scaffolds. Although the addition of 20–30% CWs in the scaffolds improved their thermal stability and resistance to biodegradation, the scaffolds with 10% CWs were the best for supporting the proliferation of cultured human osteosarcoma cells (SaOS-2).
 J Appl Polym Sci 117: 3406–3418, 2010

Key words: biomaterials; nanocomposites

INTRODUCTION

The essence of tissue engineering is aimed at generating biological substitutes for lost or defective tissues. The process of tissue regeneration requires functional scaffolding materials to serve as templates for the attachment of cells and/or mediators for subsequent tissue development.[1,2] Scaffolds, in addition to being supportive frameworks, play important roles in the transportation of nutrients, metabolites, and regulatory molecules into and wastes out of cells. They can also be functionalized to provide specific signaling to the cells.[3] To achieve isomorphous tissue replacement, materials used for fabrication into scaffolds should be biocompatible and biodegradable. Synthetic polymers, such as polylactide, polyglycolide, and their respective copolymers, have been heavily explored because of their suitable chemistry and properties that can be tailored, such that the resulting scaffolds possess a controllable mechanical integrity and *in vivo* degradability.[4–7]

Alternatively, natural polymers, such as collagen, gelatin (Gel), and alginate, have equally been studied because of their inherent hydrophilicity and the presence of certain extracellular matrix (ECM)-like properties that provide a suitable environment for cell growth.[8,9] Notwithstanding, scaffolds made from natural polymers are mechanically weak; this limits their use as regenerating templates for semi-hard and hard tissues, such as cartilage and bones. This can be improved by several means, such as crosslinking,[10–13] blending,[14,15] and chemical modification.[16,17] Here, we used blending, crosslinking, and compositing means to arrive at functional bone scaffolds with improved physical, mechanical, and biological integrities. The natural materials used to fabricate the porous scaffolds were hyaluronan (HA) and Gel, and the reinforcing fillers used to prepare the HA/Gel nanocomposite scaffolds were nanocrystalline entities obtained from the acidic hydrolysis of chitin [i.e., α-chitin whiskers (CWs)]. Both the neat and the CW-reinforced HA/Gel scaffolds were fabricated by means of a freeze-drying technique,

Additional Supporting Information may be found in the online version of this article.

**Present address:* Department of Conservative Dentistry, Faculty of Dentistry, Prince of Songkla University, Hatyai, Songkhla 90112, Thailand.

Correspondence to: P. Supaphol (pitt.s@chula.ac.th).

Contract grant sponsor: Ratchadaphisek Somphot Endowment Fund (Chulalongkorn University).

Contract grant sponsor: Center for Petroleum, Petrochemicals, and Advanced Materials (Chulalongkorn University).

Contract grant sponsor: Petroleum and Petrochemical College (Chulalongkorn University).

Contract grant sponsor: Thailand Research Fund; contract grant number: DBG5280015.

and the obtained scaffolds were characterized for their mechanical, physicochemical, and biological properties.

HA, a linear polysaccharide, contains a repeating disaccharide unit of *N*-acetyl-D-glucosamine and glucuronic acid that is linked by a β-1,4-glycosidic bond, and the disaccharides are, in turn, linked by β-1,3-bonds to from a high-molecular-weight HA chain.[18] HA belongs to a group of polysaccharides found in the ECM of connective tissues of humans; hence, terms such as *connective tissue polysaccharides, mucopolysaccharides,* and *glycosaminoglycans* have been coined to represent the polymers in this group.[19] The functions of HA as an ECM component are plenty, with the most important ones as supporting frameworks for the attachment of cells and as a mediator for promoting cellular mobility, proliferation, and differentiation.[20] Because of its chemical specificity and long-chain nature, HA provides specific binding sites for numerous proteins, proteoglycans, and other biomolecules, such as growth factors.[8] Moreover, it is a major lubricating material found between bone joints.[21] On the basis of these reasons, the blending of HA with another biopolymer is a means of developing scaffolds with superior properties to those of the precursor materials.[14,22–24]

Gel is a natural biopolymer, prepared by the partial hydrolysis of collagens, the most abundant structural proteins found in various parts of animal and human tissues. Depending on the method by which the collagens are pretreated, two types of Gel can be produced.[25,26] Acidic treatment is appropriate for the un-fully-crosslinked collagens found in porcine or fish skins (i.e., type A Gel), whereas alkaline treatment is suitable for the more fully crosslinked collagens found in bovine hides (i.e., type B Gel). The resulting Gel products are different in both their molar mass and electrical properties from the ones obtained from the alkaline treatment, which possess a greater proportion of carboxyl groups, which render them negatively charged and lower their isoelectric points compared to those obtained from the acidic treatment.[25] Structurally, Gel is a heterogeneous mixture of single- or multiple-stranded polypeptides (and their oligomers), each of which contains about 300–4000 amino acid residues.[25,26] It has been studied extensively in the fields of controlled drug release and tissue engineering. The blending of chitosan, Gel, and HA in a certain proportion enhanced the resistance to enzymatic degradation and promoted fibroblastic migration and proliferation.[27] Similarly, scaffolds made from blends of Gel, chondroitin, and HA supported the differentiation of chondrocytes that had been cultured for 5 weeks particularly well.[28]

Chitin or poly(*N*-acetyl-D-glucosamine) is a high-molecular-weight polysaccharide predominantly found in the exoskeletons of arthropods and the internal flexible backbones of cephalopods. It is nontoxic, odorless, biocompatible with living tissues, and biodegradable.[29] CWs, nanocrystalline entities of chitin, have been successfully prepared from crab shells,[30] squid pens,[31] and tubes of *Riftia pachyptila* tube worms.[32] The commonly used hydrolytic condition for obtaining CWs is 3*N* hydrochloric acid (HCl) at boiling for 90 min under vigorous stirring.[30,32] CWs have been shown to be an effective reinforcing filler for many types of polymer matrices.[31–34] Nanocomposite films of poly(vinyl alcohol)/CWs and chitosan/CWs with or without heat treatment have been successfully prepared and reported.[33,34] The CW content ranged between 0 and 29.6% (by weight of the matrix materials). The tensile strengths of the nanocomposite films were found to increase compared to those of the corresponding neat films, with an initial increase in the CW content either leveling off or reaching a maximum value at a CW content of about 2.96%.[33,34] On the other hand, significant improvements were observed in the shear modulus of a CW-reinforced copolymer of styrene and butyl acrylate[31] and in the Young's modulus of CW-reinforced polycaprolactone.[32]

EXPERIMENTAL

Materials

Chitin powder (crab shells, α form, weight-average molecular weight = 4×10^5 g/mol) was purchased from Fluka (St. Gallen, Switzerland). Gel (porcine skin, type A, 170–180 bloom) was purchased form Fluka. HA (weight-average molecular weight = 1.4×10^6 g/mol) was purchased from Coach Industries (Osaka, Japan). 1-Ethyl-3-(3-dimethylaminopropyl)carbodiimide (EDC) was purchased form Fluka. HCl [37% (w/w), analytical-reagent grade] was purchased from Labscan Asia (Bangkok, Thailand). All other chemicals were analytical-reagent grade and were used without further purification.

Preparation of the CWs

CWs were prepared by the acid hydrolysis of chitin powder with 3*N* HCl at 120°C for 6 h under vigorous stirring and refluxing. The ratio of HCl to chitin powder was 30 mL/g. After acid hydrolysis, the obtained CW suspensions were diluted with distilled water and were then centrifuged at 10000 rpm for 5 min and decanted in triplicate. The suspensions were then transferred to dialysis bags and dialyzed in running water for 2 h and later in distilled water for 2 days. The dispersion of CWs was completed by a 5-min ultrasonification treatment for every 40 mL aliquot. The solid fraction of the as-prepared CW

suspensions was gravimetrically determined to be 1.43 wt % on average. The CW suspensions were stored at 4°C before further use.

Preparation of the neat HA–Gel scaffolds and the CW-reinforced HA–Gel scaffolds

An equal mass of HA and Gel powder was first mixed and dissolved in deionized (DI) water at 50°C to obtain a blend solution of the polymers (i.e., HA–Gel) at a fixed concentration of 2 wt %. The blend solution was left to cool to room temperature before various amounts of the as-prepared CW suspensions were added to the solution. The six different mass ratios between the CWs and HA–Gel were 0, 2, 5, 10, 20, and 30% (w/w). The mixtures were continuously stirred until they were fully homogenized. To crosslink HA–Gel, 1 mmol of EDC was added, and the mixtures were further stirred for 2 h at room temperature. Volumes of the mixtures were poured into polypropylene dishes to obtain molding specimens of two different shapes and dimensions (i.e., cylindrical and disc shapes), frozen at −40°C for 24 h, and lyophilized at −50°C for another 24 h. The obtained cylindrical scaffolds were about 10 mm in diameter and 2 mm in height, whereas the disc-shaped scaffolds were about 1 mm in thickness; these were later cut into a desired shape and size for the mechanical property assessment. The as-prepared scaffold specimens were kept in a desiccator before further use.

Characterization

Microstructure observation and pore size determination

One cylindrical scaffold was randomly selected from each group of the scaffolds. It was cut into pieces along both the longitudinal and the transverse directions. The cut pieces were mounted on copper stubs, coated with gold with a JEOL JFC-1100 sputtering device (Tokyo, Japan) and observed for their microscopic structure with a JEOL JSM-5200 scanning electron microscope. To determine the dimensions of the pores, 50 pores for each of the cross sections and the longitudinal sections (i.e., 100 pores in total) were directly measured from the scanning electron microscopy (SEM) images with The University of Texas Health Science Center at San Antonio (UTHSCSA) Image Tool version 3.0 software. The average values for all of the specimens investigated were calculated and reported.

Mechanical properties

For the tensile mechanical integrity, specimens ($50 \times 5 \times 1$ mm^3) were cut from the disc-shaped scaffolds. The mechanical integrity of the specimens, measured in their dry state, in terms of the tensile strength, Young's modulus, and elongation at break was assessed with a Lloyd LRX-Plus universal testing machine (West Sussex, UK) with a 10-N load cell at room temperature (26 ± 2°C). The gauge length was 30 mm, and the crosshead speed was 10 mm/min. The measurements were carried out in pentuplicate for each group of the scaffolds.

Water-retention capacity

Cylindrical scaffolds, in their dry state, were weighed and then individually immersed in DI water at room temperature. At a given time point, the specimens were taken out, blotted on a glass plate, which was set at about 45° from a horizontal baseline for 5 s to remove excessive water, and immediately weighed. The amount of water retained in the specimens was determined according to the following equation:

$$\text{Water retention}(\%) = [(W_w - W_d)/W_w] \times 100; \quad (1)$$

where W_d and W_w are the weights of the specimens before and after submersion in the water, respectively. The measurements for each group of the scaffolds were carried out in pentuplicate at different time intervals within a period of 24 h.

In vitro degradation

The *in vitro* degradation study of the scaffolds was carried under three conditions. In the first, cylindrical scaffolds were individually immersed in a 10 m*M* phosphate buffer saline (PBS) solution (pH 7.4) at room temperature without shaking for 24 h. Under the other two conditions, they were individually immersed in either PBS or bacterial collagenase at a concentration of 373 ng/mL at 37°C under shaking (70 rpm) for 24 h. After the specified time, the specimens were removed from the media, frozen at −40°C for 24 h, and lyophilized at −50°C for another 24 h. The degradability of the specimens was then quantified according to the following equation:

$$\text{Degradability}(\%) = W_t/W_i \times 100; \quad (2)$$

where W_i is the initial dry weight of the specimens and W_t is the dry weight of the specimens after each respective *in vitro* degradation assay. The measurements for each group of the scaffolds were carried out in triplicate.

Infrared (IR) spectroscopy and thermal analyses

A Thermo Nicolet Nexus 670 Fourier transform infrared (FTIR) spectrophotometer (Madison, WI)

was used to investigate the chemical functionalities of the as-prepared scaffolds by the KBr disk method. One cylindrical scaffold was randomly selected from each group of scaffolds and subsequently subjected to FTIR scanning over 32 scans at a resolution of 4 cm^{-1}. The thermal stability of the selected cylindrical scaffold specimens was assessed in terms of their degradation temperature with a PerkinElmer TGA-7 thermogravimetric analyzer (Waltham, MA) over a temperature range of 30–600°C at a heating rate of 10°C/min under a nitrogen atmosphere. The weights of the specimens ranged between 3 and 5 mg. A PerkinElmer DSC-7 differential scanning calorimeter (Waltham, MA) was used to determine the glass-transition temperature (T_g) of the scaffold specimens over a temperature range of 25–80°C at a heating rate of 10°C/min. The specimens, weighing around 5–6 mg, were subjected to a preheating run to erase their thermal history before the test.

Biological evaluation

Cell culture

Human osteosarcoma cells (SaOS-2) were cultured as a monolayer in α-minimum essential medium (α-MEM; Sigma–Aldrich, St. Louis, MO), supplemented by 10% fetal bovine serum (Biochrom, Cambridge, UK), 1% L-glutamine (Invitrogen, Carlsbad, CA), and a 1% antibiotic and antimycotic formulation containing penicillin G sodium, streptomycin sulfate, and amphotericin B (Invitrogen). The cells were maintained at 37°C in a 95% humidified atmosphere containing 5% CO_2 and passaged once every 3–4 days.

Cytotoxicity evaluation

Only the cylindrical scaffolds containing 0 and 30% CWs were used in these studies. The cytotoxicity of the scaffolds was evaluated by the indirect method with SaOS-2 as the reference cells. First, the extraction media were prepared by immersion of the scaffold specimens in 500 μL of serum-free medium (SFM; containing MEM, 1% L-glutamine, 1% lactabumin, and a 1% antibiotic and antimycotic formulation) for 24 h. Each of these extraction media was later used in the indirect cytotoxicity evaluation. SaOS-2 were cultured in wells of a 24-well culture plate at 4×10^4 cells/well in serum-containing MEM for 16 h to allow attachment of the cells to the plate. The cells were then starved with SFM for 24 h, after which time, the medium was replaced with an extraction medium. After 24 h of cell culturing in the extraction medium, a 3-(4,5-dimethylthiazol-2-yl)-2,5-diphenyl tetrazolium bromide (MTT) assay (see details in the Supporting Information) was carried out to determine the viability of the cells. The experiment was carried out in quadruplicate.

Cell attachment and cell proliferation

A primary evaluation for cell attachment was carried out by a direct morphological observation of SaOS-2 cells that had been seeded on the surface of the scaffold specimens. Only the cylindrical scaffolds containing 30% CWs were used in the study. Specifically, the cylindrical scaffold specimens were put in wells of a 24-well culture plate and sterilized with 1 mL of 70% ethanol for 30 min. They were then washed with sterilized DI water twice and later immersed in α-MEM overnight. SaOS-2 cells were then seeded on the surfaces of the specimens at 4×10^4 cells/specimen in a minimum volume of the culture medium and were allowed to attach on the surfaces for 3 h before the addition of 1.5 mL/well of the culture medium. The cells were cultivated at 37°C in a humidified atmosphere containing 5% CO_2 for 1 and 7 days, after which time, the morphology of the cultured cells was observed by SEM. After the removal of the culture medium, the cell-cultured scaffold specimens were rinsed with PBS twice, and the cells were fixed with a 3% glutaraldehyde solution, which was diluted from a 50% glutaraldehyde solution (Electron Microscopy Science, Hatfield, PA) with PBS for 30 min. The specimens were then dehydrated in graded ethanolic solutions (i.e., 30, 50, 70, and 90%) and in pure ethanol for about 2 min each. They were further dried in 100% hexamethyldisilazane (Sigma-Aldrich) for 5 min, dried in air after the removal of hexamethyldisilazane, mounted on SEM stubs, coated with gold, and finally, observed by SEM. The examinations were performed on three randomly selected scaffold specimens.

To quantify the viability of the attached and the proliferated cells, SaOS-2 cells had first been seeded or cultured on each of the four randomly selected specimens from each group of the scaffolds for 1, 24, 48, and 72 h before they were evaluated by the MTT assay at each time point. Only the cylindrical scaffolds were used in this study.

Statistical analysis

Data were analyzed with SPSS software version 14.0 for Windows (SPSS, Chicago, IL). Initially, the normal distribution was assessed by the Shapiro–Wilk test. The normal distribution data, representing the homogeneity of the variances, shown by the Levene's test, were then investigated by a one-way analysis of variance (ANOVA) with the Tukey HSD *post hoc* multiple comparisons. Otherwise, the Dunnett T3 was applied if the data did not exhibit the homogeneity of the variances. For the data of which the

normal distribution was absent but the variance was homogeneous, the Kruskal–Wallis H was applied. To compare the means between two data groups, the Student unpaired t test was used. The significant level was indicated at $p < 0.05$ in any case.

RESULTS AND DISCUSSION

Characterization of the CWs

The dialyzed CWs exhibited colloidal behavior in water. Protonation of the amino groups of chitin under acidic conditions induced positive charges (NH_3^+) on the surface of the CWs, which generated electrostatic repulsion among the nanocrystallites.[30] However, protonation of amino groups was not complete on all of the CW particles; hence, the hydrogen bonding associated with the free amino groups on the CWs caused them to aggregate. The representative TEM image of the as-prepared CWs, which were prepared from a dilute suspension, is illustrated in Figure 1. It was evident that the CWs were present as individual and partially aggregated entities. The aggregation of the CWs was facilitated by the increase in the pH of the suspension during dialysis, hence, the deprotonation of some of the protonated amino groups that occurred during the acid hydrolysis to prepare the CWs. According to the TEM results, the as-prepared CWs were present as slender rods with sharp points on both ends. The lengths (L's) and widths (d's) of these rods were 255 ± 56 and 31 ± 6 nm, respectively, with an L/d ratio of about 8. The histograms illustrating the distribution of the lengths and the widths of the as-prepared CWs, as shown in the Supporting Information, indicated that over 50% of the CWs exhibited lengths and the widths in the range 203–277 and 27–35 nm, respectively. These dimensions compared well with the reported values for CWs obtained from crab shells (L = 50–300 nm and d = 6–8 nm,[30] L = 100–600 nm and d = 4–40 nm,[35] and L = 100–650 nm and d = 10–80 nm[36]).

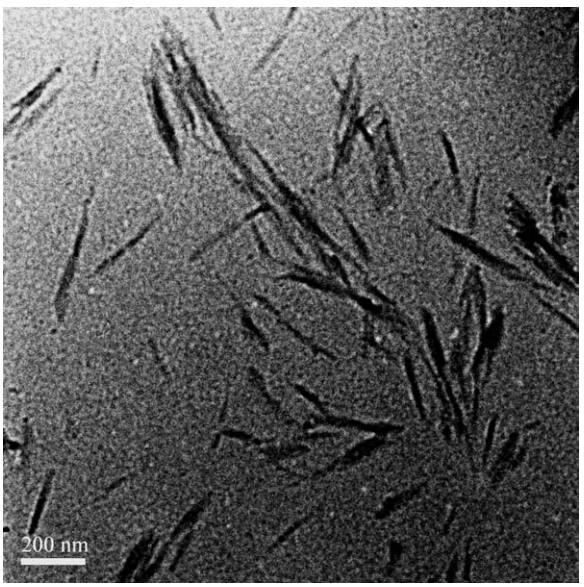

Figure 1 Representative TEM image of CWs prepared from a diluted suspension of acid-hydrolyzed chitin powder from crab shells.

Characterization of the CW-reinforced HA–Gel scaffolds

Physical characteristics

Representative photographic images of the as-prepared cylindrical scaffolds are shown in the Supporting Information. These scaffolds were extremely light in weight because of their highly porous nature. The color of these scaffolds ranged from the pure white of the neat HA–Gel scaffolds to the light brown of the 30% (w/w) CW-reinforced HA–Gel scaffolds. The brown color resulted from the presence of the CWs dispersing within the mass of the scaffolds. Representative SEM images illustrating the microstructure of the as-prepared scaffolds viewed on the surface perpendicular to the transverse direction (i.e., the surface of the transverse sections) are shown in Figure 2, whereas those illustrating the microstructure of the scaffolds viewed on the surface perpendicular to the longitudinal direction (i.e., the surface of the longitudinal sections) are shown in the Supporting Information. All of the scaffolds exhibited a well-defined porous structure, and regardless of the surface under consideration, the interpore connectivity was discernible throughout the bulk of the scaffolds. For a given group of the scaffolds, no significant difference in terms of the morphology of the pore structure was observed between the two sections. This was in exception to the one that contained 30% CWs, which showed a disruption in its microstructure when viewed on the surface of the longitudinal sections. The dimensions of the pores observed in these SEM images were determined and analyzed and are reported in Table I.

The size of the pores for all of the scaffolds in both the transverse and the longitudinal sections ranged between 92 and 230 μm, with the average value ranging between 139 and 166 μm. An increase in the content of the CWs did not have a significant effect on the pore dimensions. A comparison of the pore dimensions that were observed in the two sections for each group of the scaffolds was evaluated statistically, and there was no difference, except for those observed for the neat HA–Gel sample group. With an average pore size smaller than 200 μm, the transportation of nutrients and oxygen and the ingrowth of new blood vessels into the inner pores of the scaffolds were somewhat restricted. The lack of

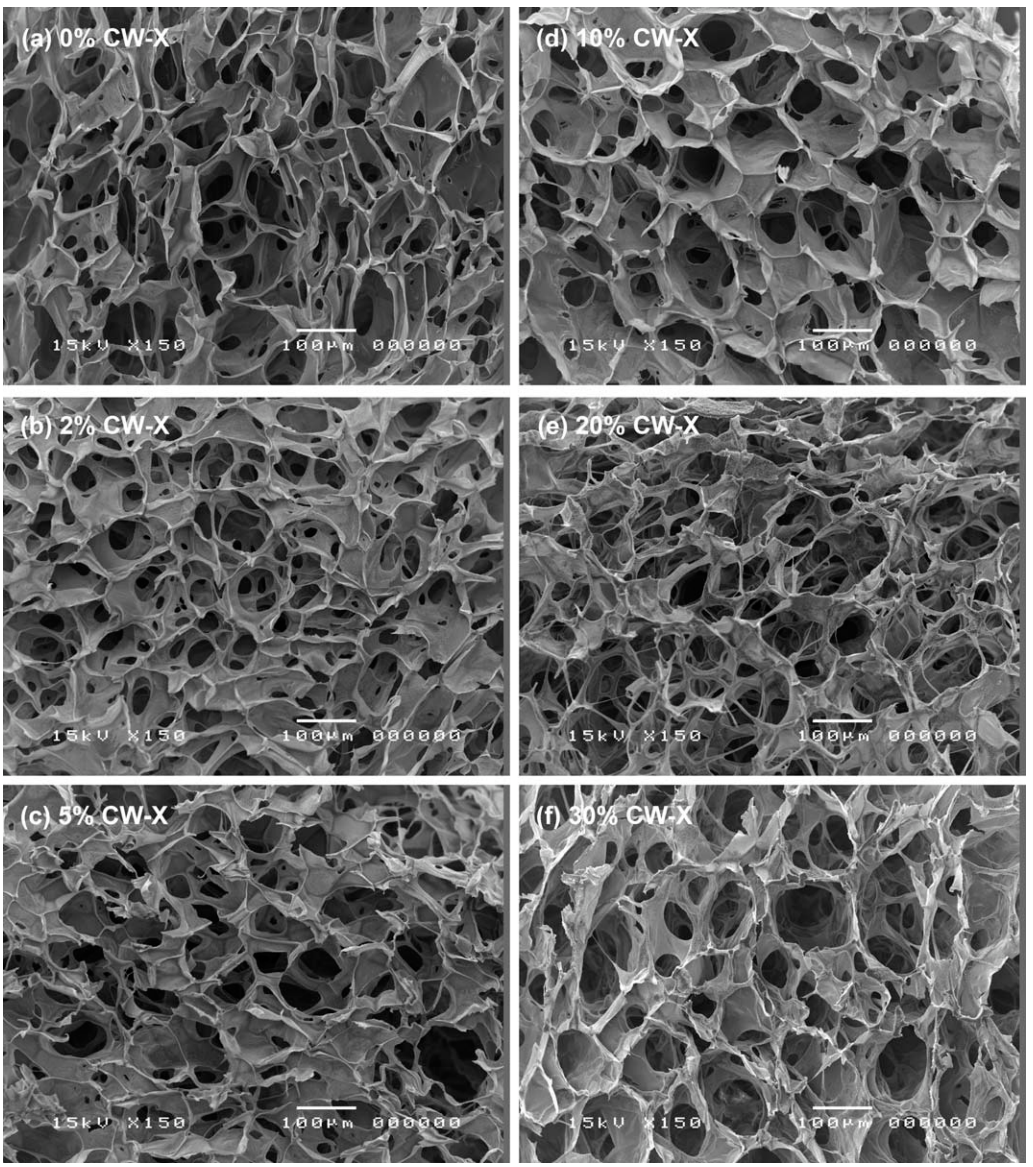

Figure 2 Representative SEM images illustrating the microstructures of the (a) neat HA–Gel scaffolds and CW-reinforced HA–Gel scaffolds containing (b) 2, (c) 5, (d) 10, (e) 20, and (f) 30% (w/w) CWs (viewed on surfaces perpendicular to the longitudinal direction, i.e., transverse surfaces).

TABLE I
Dimensions of the Pores of the Neat HA–Gel Scaffolds and the CW-Reinforced HA–Gel Scaffolds Observed on the Surfaces of Both Transverse and Longitudinal Sections

	Pore size (μm)			
	Transverse sections		Longitudinal sections	
Specimen	Range (Minimum − Maximum)	Average (Mean ± Standard deviation)	Range (Minimum − Maximum)	Average (Mean ± Standard deviation)
0% CW	92.3–208.8	140.9 ± 21.8[a]	112.8–231.4	165.8 ± 27.7[a]
2% CW	114.4–182.0	139.4 ± 16.0[b]	108.4–182.1	145.4 ± 15.3[b]
5% CW	104.1–224.5	153.2 ± 23.9[c]	110.6–171.1	142.7 ± 13.8[c]
10% CW	118.0–202.3	158.9 ± 19.1[d]	104.3–205.4	162.8 ± 23.6[d]
20% CW	113.5–200.5	151.4 ± 19.3[e]	105.8–181.0	143.9 ± 17.2[e]
30% CW	108.5–184.4	155.4 ± 15.7[f]	97.2–231.3	149.0 ± 25.1[f]

Superscript letters indicate comparisons only between sections of a given group of specimens at $p < 0.05$ (one-way ANOVA with Tukey HSD, $n = 50$).

TABLE II
Mechanical Properties of the Neat HA–Gel Scaffolds and the CW-Reinforced HA–Gel Scaffolds

Specimen	Modulus of elasticity (MPa)	Elongation at break (%)	Tensile strength (MPa)
0% CW	0.99 ± 0.10[a]	53.48 ± 10.69[a]	0.52 ± 0.06[a]
2% CW	14.10 ± 2.23[b]	28.35 ± 6.16[b]	1.03 ± 0.09[b]
5% CW	19.96 ± 3.64[b]	06.36 ± 1.42[c]	0.53 ± 0.15[a,c]
10% CW	12.46 ± 2.00[b]	11.63 ± 4.15[c,d]	0.48 ± 0.19[a,c]
20% CW	07.10 ± 0.93[c]	16.07 ± 0.96[b,d]	0.47 ± 0.06[a]
30% CW	11.96 ± 0.47[b]	16.03 ± 3.40[b,d]	0.72 ± 0.08[c]

Superscript letters indicate comparisons between groups of specimens for a single property at $p < 0.05$ (one-way ANOVA with Dunnett T3, $n = 5$).

ample oxygen supply leads to a medical condition known as *hypoxia*, which is suitable for the regeneration of cartilage but certainly not bone.[37,38] To obtain scaffolds with larger pore dimensions, the cooling rate associated with the freezing of the HA–Gel solution or the HA–Gel/CWs suspensions before the subsequent sublimation of the ice crystals needs to be decreased further because it is a known fact that a fast cooling rate induces the formation of tiny ice crystals, hence, the small pore dimensions.[39,40]

Mechanical properties

Mechanical properties, expressed in terms of the modulus of elasticity, elongation at break, and tensile strength, of the as-prepared scaffolds were evaluated, and the results are summarized in Table II. Statistical analysis indicated that inclusion of the CWs in amounts of 2–30% in the HA–Gel scaffolds resulted in a significant increase in the modulus of elasticity from that of the neat scaffolds. Nevertheless, the property values among the various groups of the CW-reinforced HA–Gel scaffolds were not statistically different, except for the one containing 20% CWs, which showed significantly lower values. For the elongation at break, the neat HA–Gel scaffolds exhibited significantly greater values over all of the reinforced samples, which statistically showed equivalent values among themselves. With regard to the tensile strength, it was obvious that the HA–Gel scaffolds that contained 2% CWs exhibited the property values that were significantly greater than those of the other groups of samples, which, among themselves, showed equivalent values. The result agreed well with the report of Sriupayo et al.,[34] who found that the greatest tensile strength of CW-reinforced chitosan films was observed at a CW content of 2.96% and an increase in the CW content resulted in a reduction in the property values. To put it into perspective, the modulus of elasticity and the tensile strength values of the scaffolds containing 2% CWs were much lower than those of bone, which are 16.4 GPa and 117.4 MPa, respectively, on average.[41]

Water absorption and *in vitro* degradability

The ability of the neat and CW-reinforced HA–Gel scaffolds to absorb water at room temperature within 24 h is graphically shown in Figure 3. All groups of the scaffolds demonstrated comparable water absorption within the first 60 min, which accounted for more than about 95% of their total wet weights. The values were as high as that of a superabsorbent.[42] The results were similar to those reported by Park et al.[43] on collagen–HA sponges. Such a great tendency to absorb a great amount of water is characteristic of a hydrogel material, such as HA and Gel, which are very hydrophilic in nature.[9] With the absorbed water, the interior of a scaffold becomes a hydrated environment, which facilitates the process of tissue regeneration by protecting cells and their products, such as secreted ECM. Furthermore, the hydrated environment facilitates the transportation of nutrients into and wastes out of the cells.[24] According to Figure 3, all groups of the scaffolds exhibited similar water absorption values and equivalent profiles; that is, the property values decreased gradually with increasing submersion time. The absorption of water in a given group of the scaffolds reached a maximum only after having been submerged in DI water for 15 min, and the inclusion of the CWs within the scaffolds did not strongly influence the water absorption. This was due to the inherent hydrophilicity of all of the compositions, the interconnectivity of the pore structures, and the similarity in the pore dimensions of all of the scaffolds, which facilitated the capillary

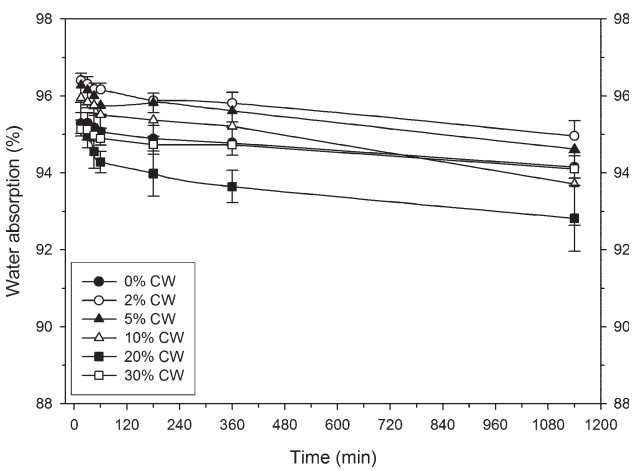

Figure 3 Ability of the neat HA–Gel scaffolds and the CW-reinforced HA–Gel scaffolds to absorb DI water (shown as the amount of water absorbed) at room temperature as a function of the submersion time.

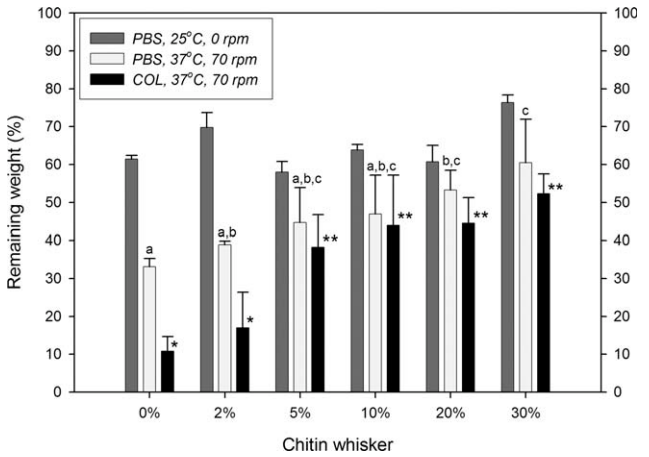

Figure 4 Degradability of the neat HA–Gel scaffolds and the CW-reinforced HA–Gel scaffolds (shown as the remaining weights of the scaffolds) in a PBS solution under static conditions (at 25°C without agitation) or dynamic conditions (at 37°C with agitation at 70 rpm) and in an aqueous solution of collagenase (COL) (at 37°C with agitation at 70 rpm) as a function of the CW content for the total observation period of 24 h. $^{a,b,c,*}p < 0.05$ (one-way ANOVA with Tukey HSD, $n = 4$).

action and, hence, the rapid adsorption of water.[42] The observed decrease in the amounts of water absorbed as the immersion time increased might have been due to the fact that the scaffolds began to disintegrate or partially dissolve, which diminished their capacity to imbibe both free and bound water.[24,43]

Despite the many benefits of the high water absorption of a scaffold, certain drawbacks should also be considered, such as weakening and acceleration due the to degradation of the scaffold.[24] The degradation of a scaffold occurs mainly by either a physical or chemical pathway. The physical pathway involves dissolution and hydrolysis, whereas the chemical pathway involves enzymatic cleavage in the presence of a suitable enzyme.[9] Here, we investigated the dissolution and hydrolytic degradation of the scaffolds in PBS over a submersion period of 24 h under both static conditions at room temperature and dynamic conditions, that is, by means of a shaking water bath at 70 rpm and 37°C. The enzymatic degradation of the scaffolds was also investigated in 373 ng/mL of bacterial collagenase, which represented a model concentration of tissue collagenase in the synovial fluid of the patients with osteoarthritis.[44,45] The investigation was carried out in the shaking water bath at 70 rpm and 37°C for 24 h. The results of these studies are graphically shown in Figure 4.

Figure 4 shows the remaining weights of the scaffolds after submersion in PBS or collagenase (COL) solution for 24 h. Upon submersion in PBS under the static conditions at room temperature, the remaining weights of the scaffolds were about 58–76% of their original dry weights, with no significant difference among all groups of the scaffolds. Under the dynamic conditions, on the other hand, the remaining weights, for a given group of the scaffolds, were significantly lower than those observed under the static conditions. The enhancement in the weight loss was obviously due to the added energy from the agitation, which increased the kinetic energy of the system. In addition, the thermal degradation of the HA molecules could occur to a certain extent at 37°C.[18] These could have been factors contributing to the observed values of the remaining weights of the scaffolds at 33–60% of the original dry weights of the scaffolds. The incorporation of CWs in the amounts of 20–30% in the HA–Gel scaffolds enhanced the resistance to degradation under the dynamic conditions compared with the neat scaffolds. Although a trend was observed for the relationship between the remaining weights of the scaffolds and the CW content, statistical analysis among the scaffolds that contained 5–30% CWs did not show a significant difference in their property values.

In the collagenase medium, the degradation of the scaffolds was noticeably enhanced as the remaining weights, for a given group of the scaffolds, were the lowest. Regardless of the CW content, the values were in the range 11–52% of the original dry weights of the scaffolds. In addition to the agitation and the hypothetical thermal degradation of HA, the scission of Gel peptide bonds at glycine subunits by the enzyme was the main contributing factor.[43] The presence of the CWs at levels of 5% or more significantly enhanced the stability to degradation of the scaffolds in the presence of the enzyme. Such an enhancement could have been due to the interaction between the CWs and the HA–Gel matrix molecules, which reduced the enzyme accessibility.[46]

IR spectroscopy analysis

Figure 5 illustrates FTIR spectra of the neat and CW-reinforced HA–Gel scaffolds over the wave-number range 3500–500 cm^{-1}. Those of the constituting materials are also shown for comparison. The absorption peaks at 1656, 1547, 1450, and 1237 cm^{-1}, characteristic of amide bonds (CO—NH), were observed in the spectrum of Gel,[43,47,48] whereas those at 1412 and 1076 cm^{-1}, corresponding to carboxylate salts (symmetric stretching) and ester bonds, respectively, were observed in the spectrum of HA, of which repeating units comprised glucuronic acid and acetylglucosamine. The spectrum of the CWs should have been similar to that of HA because both of them were polysaccharides. Being crystalline entities, however, the CWs presented sharper and more intense signals at certain positions,[49] particularly at 1076 (ester bonds), 1378

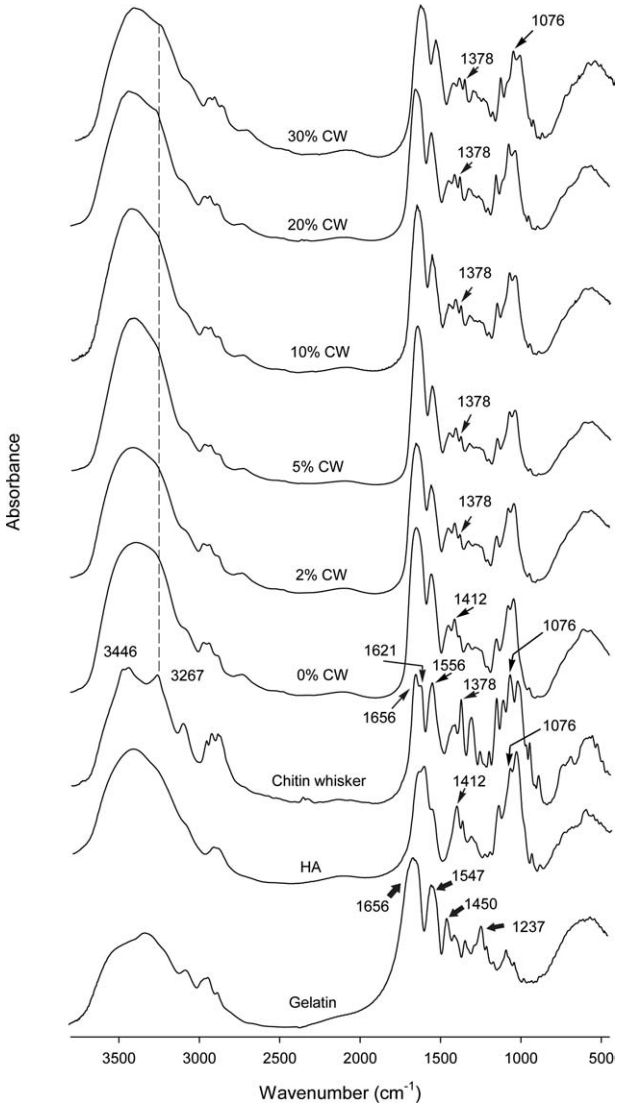

Figure 5 IR spectra of the Gel, HA, CWs, and corresponding scaffolds.

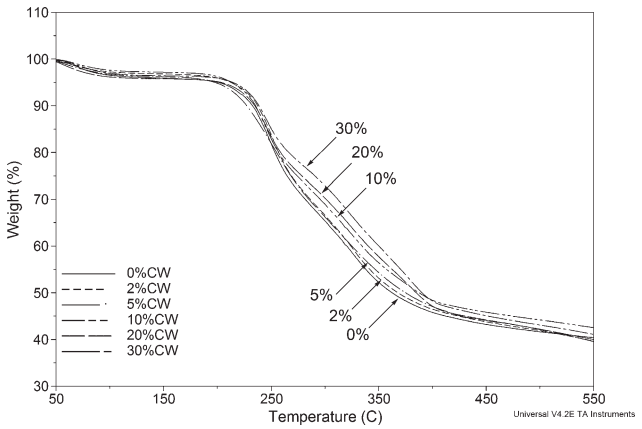

Figure 6 Thermogravimetric analysis thermograms (10°C/min in a nitrogen atmosphere) of the neat HA–Gel scaffolds and the CW-reinforced HA–Gel scaffolds.

(carboxylate salts), and 3267 and 3446 cm^{-1} (hydroxyl groups).[48] Additionally, the CWs exhibited characteristic amide I peaks at 1621 and 1656 cm^{-1} and the amide II peak at 1556 cm^{-1}.[35,47] The peak at 1621 cm^{-1} was only specific to CWs, whereas that at 1656 cm^{-1}, representing the stretching of hydrogen bonds between carbonyl groups and the neighboring amine groups of intrachains, could also be found for the amide bonds of a protein.[49]

For the neat HA–Gel scaffolds, the peaks at 1650, 1550, 1412, and 1076 cm^{-1} were discernible. Crosslinking with EDC generated both the amide and the ester linkages in the structure of the blends.[50] The amide bonds were formed between the carboxyl groups of Gel and/or of the glucuronic acid in HA and the amino groups of Gel. The ester bonds, on the other hand, were formed between the carboxyl groups and the hydroxyl groups of Gel and/or of HA.[51,52] For the scaffolds that contained CWs, the presence of the CWs were confirmed by the presence of characteristic peaks at 1378 and 1076 cm^{-1} and the absorption shoulder at 3267 cm^{-1}, and the intensities of these peaks and the shoulder were found to increase with an increase in the content of the CWs.

Thermal characteristics

Figure 6 shows thermogravimetric analysis thermograms of the as-prepared scaffolds. All samples exhibited similar profiles of weight change. Table III summarizes the values of the temperatures at which the losses in the weight of the scaffolds reached 5, 25, and 50% (on the basis of their original weights). Apparently, at temperatures lower than 200°C, the loss in the weight of all of the scaffolds, except for the ones containing 5% CWs, was less than 5%, with no particular relationship with the CW content. At temperatures around 210–230°C, the loss in the weight increased abruptly to reach maximum values at temperatures around 245–250°C, as indicated by the positions of the peaks of the corresponding

TABLE III
Temperatures at Which 5, 25, and 50% Mass Losses Were Reached (T-5%, T-25%, and T-50%, respectively) for the Neat HA–Gel scaffolds and the CW-Reinforced HA–Gel Scaffolds and Residual Weights at 550°C

Specimen	T-5% (°C)	T-25% (°C)	T-50% (°C)	Residue at 550°C (wt %)
0% CW	200.6	264.9	362.6	40.4
2% CW	212.6	269.0	368.0	39.6
5% CW	194.4	268.4	375.0	39.6
10% CW	213.3	274.2	387.8	42.5
20% CW	203.3	278.5	385.0	40.0
30% CW	214.4	290.7	390.5	41.1

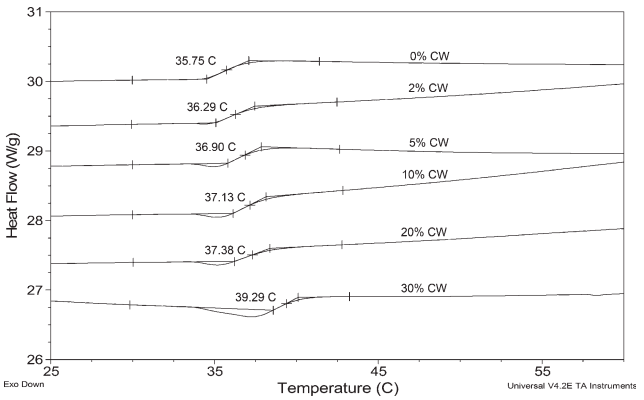

Figure 7 Differential scanning calorimetry thermograms (10°C/min in a nitrogen atmosphere) of the neat HA–Gel scaffolds and the CW-reinforced HA–Gel scaffolds. Their T_g's are illustrated.

derivative curves (not shown). As the temperatures increased to around 260–360°C, the loss in the weight of the different groups of the scaffolds became most noticeably different and inversely related to the CW content within the scaffolds. Careful consideration of the results revealed that the temperatures required for the scaffolds that contained 10–30% CWs to reach 25 and 50% of the weight loss were significantly greater than those of the neat scaffolds and the ones containing 2 and 5% CWs. This demonstrated that reinforcing the scaffolds with 10–30% CWs enhanced the thermal stability of the resulting scaffolds. Notwithstanding, such enhancement was only reflected in a limited temperature range, that is, 260–360°C, as the residual weights of all of the scaffolds at 550°C were comparable.

Figure 7 shows the differential scanning calorimetry thermograms of the as-prepared scaffolds. The range of the temperature was chosen such that it revealed the glass transitions of the materials. Apparently, the neat HA–Gel scaffolds exhibited the T_g at about 35.8°C. With the addition and increasing amount of the CWs, T_g was found to increase from that of the neat materials to 36.3°C at 2% CWs and finally to 39.3°C at 30% CWs. With the T_g values of the HA–Gel scaffolds that contained 5–30% CWs in the range 36.9–39.3°C, the enhancement in the resistance to biodegradation of the corresponding scaffolds by collagenase, as previously shown, could have been, at least partly, due to the observed increase in the T_g values from that of the neat materials. The increased T_g values that were close to or greater than the physiological temperature of 37°C should have resulted in less mobility of the matrix molecules and, thus, the lower tendency for conformational change. However, because the T_g values of these scaffolds were measured in their dry state, the actual values in the physiological environment (i.e., wet conditions) should be much less because of the plasticizing effect from absorbed water molecules. Nevertheless, the marked increase in the T_g values for the scaffolds that contained 5–30% CWs coincided with the observed improvement in the resistance to enzymatic degradation of these scaffolds.

Cytotoxicity and *in vitro* response of bone cells

We first investigated the cytotoxicity of the as-prepared scaffolds. The assessment was carried out on the basis of the indirect cytotoxicity assay, in which the extraction media from the neat and the 30% CW-reinforced HA–Gel scaffolds were used to incubate SaOS-2 osteosarcoma cells for 24 h. The viability of the cells, determined spectrophotometrically at 570 nm, was compared with that of the cells that had been incubated with SFM for the same period of time. The results are shown in Table IV. Evidently, the viability of the cells that were cultured with either the extraction media from the neat scaffolds or the SFM was statistically the same, a result indicating that the neat HA–Gel scaffolds were biocompatible with the bone cells. Nevertheless, the viability of the cells decreased significantly when they were cultured with the extraction media form the scaffolds that contained 30% CWs. This result suggests that the presence of the CWs (at 30%) had an adverse effect on cell viability. Further evaluation by the direct culturing of the cells onto the scaffolds was then carried out to confirm whether they were toxic to the cells.

Figure 8 shows representative SEM images in various magnifications of SaOS-2 cells that were cultured on the surfaces of the 30% CW-reinforced HA–Gel scaffolds for 1 or 7 days. On day 1, the cells attached well to the surfaces of the scaffolds. The majority of the cells exhibited evidence of cytoplasmic process in the form of filopodia over the

TABLE IV
Indirect Cytotoxicity Evaluation of the Neat HA–Gel Scaffolds and the 30% CW-Reinforced HA–Gel Scaffolds on the Basis of the Viability of Human Osteosarcoma Cells (SaOS-2)

	Absorbance at 570 nm		
Sample	Control	0% CW	30% CW
1	0.575	0.524	0.465
2	0.508	0.536	0.410
3	0.537	0.487	0.409
4	0.540	0.569	0.428
Average	0.540 ± 0.027	0.529 ± 0.034	0.428 ± 0.026*

* At $p < 0.05$ (one-way ANOVA with Tukey HSD, $n = 4$).

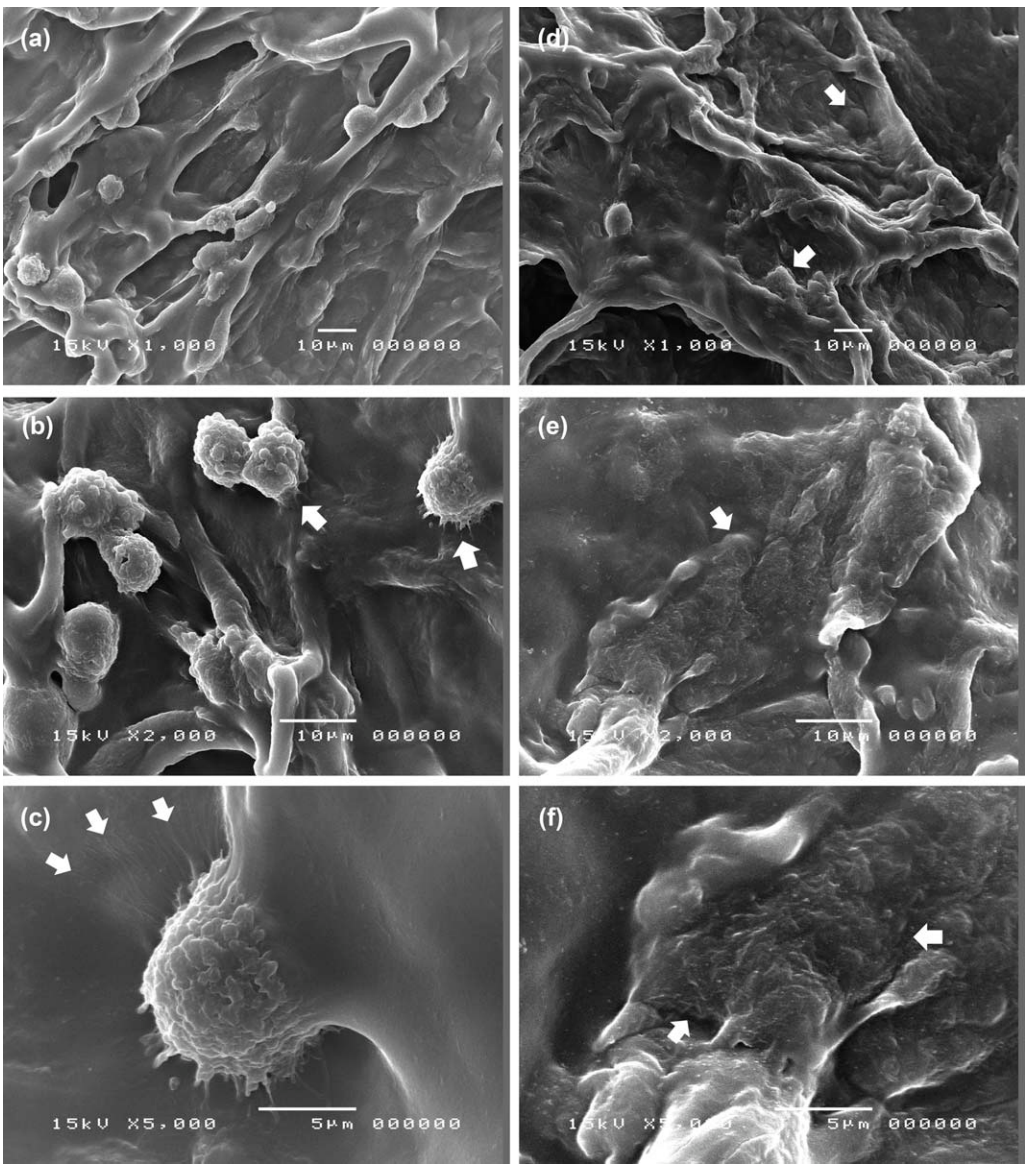

Figure 8 Representative SEM images at different magnifications [(a,d) 1000, (b,e) 2000, and (c,f) 5000×] illustrating the morphology and behavior of SaOS-2 cultured on the surfaces of 30% CW-reinforced HA–Gel scaffolds for (a–c) 1 and (d–f) 7 days. White arrows show (b,c) the cytoplasmic process of the cells and (d–f) cells that fused into the underlying surfaces of the scaffolds.

surfaces [see Fig. 8(b,c), as indicated by arrows]. The observation of cytoplasmic expansion indicated a good initial response of the cells to the as-prepared scaffolds, which influenced the subsequent cellular processes of proliferation and differentiation.[53] On day 7, the morphology of the cells changed from the rather well-defined round shape observed on day 1 to fully expanded and even fused to the underlying surfaces of the scaffolds [see Fig. 8(d–f), as indicated by arrows]. Such an observation confirmed the preference of the cells to the surfaces, as they adhered and spread well over the surfaces. Despite the fact that the indirect cytotoxicity evaluation of the studied scaffolds produced a poor result, the observation of the bone cells that appeared to attach and expanded well over their surfaces indicated the applicability of the scaffolds for bone cell culture.

To investigate the effect of CW content on the proliferation of bone cells, the viability of SaOS-2 cells that were cultured on the neat and CW-reinforced HA–Gel scaffolds for 1, 24, 48, and 72 h was evaluated by the MTT assay. The results are graphically shown in Figure 9. At 1 h after cell seeding, the viability of the adherent cells on the surfaces of the scaffolds was either as good as or better than that on the tissue culture plate. At 24 h after cell culturing, only the cells that had been cultured on the surfaces of the 10% CW-reinforced HA–Gel scaffolds showed viability greater than the other groups of the scaffolds and the tissue culture plate. At 48 and 72 h

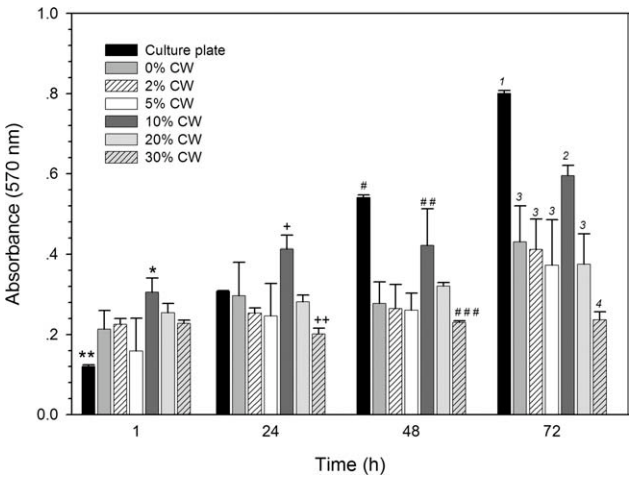

Figure 9 Viability of SaOS-2 cultured on the surfaces of the neat HA–Gel scaffolds and the CW-reinforced HA–Gel scaffolds. $^{*,+,\#,1}p < 0.05$ (one-way ANOVA with Tukey HSD, $n = 4$).

after cell culturing, the viability of the cells on the tissue culture plate was significantly greater than that of those cultured on the surfaces of the scaffolds. Among the various groups of the scaffolds, the ones containing 10% CWs, again, exhibited the greatest viability of the cultured bone cells. It has been suggested that the presence of HA is not always positive in regulating the functions of cells.[54] Liu et al.[27] reported that HA–Gel–chitosan ternary blend films with a weight content of HA of 0.31% significantly promoted the attachment, migration, and proliferation of fibroblasts better than those with weight contents of HA of 1.56 and 3.11%. On the basis of these negative reports, the composition of HA within the scaffolds could be reduced to establish a much better positive environment for cell culture. Notwithstanding, among the various groups of the scaffolds, the ones that contained 10% CWs showed the most promising results for the attachment and proliferation of the bone cells.

CONCLUSIONS

CW-reinforced HA–Gel nanocomposite scaffolds were successfully fabricated by the freeze-drying method. The variation in the amount of the incorporated CWs did not have an obvious effect on the morphology of the internal structure of the scaffolds. Nevertheless, the characteristics of the as-prepared scaffolds could be regulated through the variation in the amount of the incorporated CWs so that the optimal balance among their physicochemical, mechanical, and biological properties could be achieved. A high proportion of incorporated CWs was found to enhance the thermal stability and the resistance to biodegradation, whereas a rather low proportion of the CWs increased the tensile strength and enhanced the biocompatibility in terms of the attachment and proliferation of the cultured human osteosarcoma cells of the resulting scaffolds. Although the scaffolds that contained 10% CWs showed great promise as substrates for bone cell culture, their actual utilization could be limited to a low-stress-bearing area, such as the socket of a dental root.

The authors thank Prasit Pavasant (Faculty of Dentistry, Chulalongkorn University) for access to the cell culture facility and Tanom Bunaprasert (Faculty of Medicine, Chulalongkorn University) for fruitful discussion.

References

1. Rezwan, J. K.; Chen, Q. Z.; Blanker, J. J.; Boccaccini, A. R. Biomaterials 2006, 27, 3413.
2. Griffith, L. G. Acta Mater 2000, 48, 263.
3. Vunjak-Novakovic, G. In Culture of Cells for Tissue Engineering; Vunjak-Novakovic, G.; Freshney, R. I., Eds.; Wiley: Hoboken, NJ, 2006; p 132.
4. Mathew, H. W. T. In Polymeric Biomaterials; Dumitriu, S., Ed.; Marcel Dekker: New York, 2002; p 168.
5. Mercier, N. R.; Costantino, H. R.; Tracyc, M. A.; Bonassar, L. J. Biomaterials 2005, 26, 1945.
6. Wu, L.; Ding, J. Biomaterials 2004, 25, 5821.
7. Wu, C. S.; Liao, H. T. Polymer 2005, 46, 10017.
8. Alberts, B.; Johnson, A.; Lewis, J.; Raff, M.; Roberts, K.; Walter, P. Molecular Biology of the Cell, 4th ed.; Garland Science: New York, 2002.
9. Drury, L. J.; Mooney, D. J. Biomaterials 2003, 24, 4337.
10. Lee, K. Y.; Rowley, J. A.; Eiselt, P.; Moy, E. M.; Bouhadir, K. H.; Mooney, D. J. Macromolecules 2000, 33, 4291.
11. Shu, X. Z.; Liu, Y.; Palumbo, F.; Prestwich, G. D. Biomaterials 2003, 24, 3825.
12. Segura, T.; Anderson, B. C.; Chung, P. H.; Webber, R. E.; Shull, K. R.; Shea, L. D. Biomaterials 2005, 26, 359.
13. Liu, Y.; Shu, X. Z.; Prestwich, G. D. Biomaterials 2005, 26, 4737.
14. Liu, L. S.; Thompson, A. Y.; Heidaran, M. A.; Poser, J. W.; Spiro, R. C. Biomaterials 1999, 20, 1097.
15. Wong, M.; Siegrist, M.; Wang, X.; Hunziker, E. J Orthop Res 2001, 19, 493.
16. Prestwich, G. D.; Marecak, D. M.; Marecek, J. F.; Vercruysse, K. P.; Ziebell, M. R. J Controlled Release 1998, 53, 93.
17. Shu, X. Z.; Liu, Y.; Palumbo, F. S.; Luo, Y.; Prestwich, G. D. Biomaterials 2004, 25, 1339.
18. Lapcik, L. J.; Lapcik, L.; Smedt, S. D.; Demeester, J.; Chabrecek, P. Chem Rev 1998, 98, 2663.
19. Mano, J. F.; Silva, G. A.; Azevedo, H. S.; Malafaya, P. B.; Sousa, R. A.; Silva, S. S.; Boesel, L. F.; Oliveira, J. M.; Santos, T. C.; Marques, A. P.; Neves, N. M.; Reis, R. L. J R Soc Interface 2007, 4, 999.
20. Kikuchi, T.; Yamada, H.; Fujikawa, K. Osteoarthr Cartil 2001, 9, 351.
21. Mikos, A. G.; Lu, L.; Temenoff, J. S.; Tessmar, J. K. In Biomaterials Science: An Introduction to Materials in Medicine, 2nd ed.; Schoen, F. J.; Lemons, J. E., Eds.; Elsevier: New York, 2004; p 735.
22. Oerther, S.; Payan, E.; Lapicque, F.; Presle, N.; Hubert, P.; Muller, S.; Netter, P.; Lapicque, F. Biochim Biophys Acta Gen Subj 1999, 1426, 185.
23. Oerther, S.; Le Gall, H.; Payan, E.; Lapicque, F.; Presle, N.; Hubert, P.; Dexheimer, J.; Netter, P.; Lapicque, F. Biotechnol Bioeng 1998, 63, 206.

24. Hoffman, A. S. Adv Drug Delivery Rev 2002, 43, 3.
25. Young, S.; Wong, M.; Tabata, Y.; Mikos, A. G. J Controlled Release 2005, 109, 256.
26. Tabata, Y.; Nagano, A.; Muniruzzaman, M.; Ikada, Y. Biomaterials 1998, 19, 1781.
27. Liu, H.; Yin, Y.; Yao, K.; Ma, D.; Cui, L.; Cao, Y. Biomaterials 2004, 25, 3523.
28. Chang, C. H.; Liu, H. C.; Lin, C. C.; Chou, C. H.; Lin, F. H. Biomaterials 2003, 24, 4853.
29. Ravi Kumar, M. N. V. React Funct Polym 2000, 46, 1.
30. Revol, J. F.; Marchessault, R. H. Int J Biol Macromol 1993, 15, 329.
31. Paillet, M.; Dufresne, A. Macromolecules 2001, 34, 6527.
32. Morin, A.; Dufresne, A. Macromolecules 2002, 35, 2190.
33. Sriupayo, J.; Supaphol, P.; Blackwell, J.; Rujiravanit, R. Polymer 2005, 46, 5637.
34. Sriupayo, J.; Supaphol, P.; Blackwell, J.; Rujiravanit, R. Carbohydr Polym 2005, 62, 130.
35. Nair, K. G.; Dufresne, A. Biomacromolecules 2003, 4, 657.
36. Lu, Y.; Weng, L.; Zhang, L. Biomacromolecules 2004, 5, 1046.
37. Boyan, B. D.; Hummert, T. W.; Dean, D. D.; Schwartz, Z. Biomaterials 1996, 17, 137.
38. Karageorgiou, V.; Kaplan, D. Biomaterials 2005, 26, 5474.
39. Kang, H. W.; Tabata, Y.; Ikada, Y. Biomaterials 1999, 20, 1339.
40. Shapiro, L.; Cohen, S. Biomaterials 1997, 18, 583.
41. Currey, J. J Theor Biol 2004, 231, 569.
42. Park, H.; Park, K. In Hydrogels and Biodegradable Polymers for Bioapplications; Ottenbrite, R. M.; Huang, S. J.; Park, K., Eds.; American Chemical Society: Washington, DC, 1994; p 1.
43. Park, S. N.; Park, J. C.; Kim, H. O.; Song, M. J.; Suh, H. Biomaterials 2002, 23, 1205.
44. Maeda, S.; Sawai, T.; Uzuki, M.; Takahashi, Y.; Omoto, H.; Seki, M.; Sakurai, M. Ann Rheum Dis 1995, 54, 970.
45. Holland, T. A.; Tabata, Y.; Mikos, A. G. J Controlled Release 2005, 101, 111.
46. Vizarova, K.; Bakos, D.; Rehakova, M.; Perikova, M.; Panakova, E.; Koller, J. Biomaterials 1995, 16, 1217.
47. Magoshi, J.; Mizuide, M.; Magoshi, Y. J Polym Sci Polym Phys Ed 1979, 17, 515.
48. Coates, J. In Encyclopedia of Analytical Chemistry; Meyers, R. A., Ed.; Wiley: Chichester, England, 2000; p 10815.
49. Rinaudo, M. Prog Polym Sci 2006, 31, 603.
50. Prestwich, G. D. Biomaterials from Chemically-Modified Hyaluronan. http://www.glycoforum.gr.jp/science/hyaluronan/HA18/HA18E.html (accessed Jan 2010).
51. Sannino, A.; Papada, S.; Madaghiele, M.; Maffezzoli, A.; Ambrosio, L.; Nicolais, L. Polymer 2005, 46, 11206.
52. Tomihata, K.; Ikada, Y. J Biomed Mater Res 1997, 37, 243.
53. Anselme, K. Biomaterials 2000, 21, 667.
54. Stern, R.; Asari, A. A.; Sugahara, K. N. Eur J Cell Biol 2006, 85, 699.